THE ASTROPHYSICAL JOURNAL, 390:550–559, 1992 May 10

THE ROTATION OF M DWARFS

GEOFFREY W. MARCY[1]
Astronomy Department, University of California, Berkeley
AND
GRACE H. CHEN
Department of Physics, Massachusetts Institute of Technology, Cambridge, MA 02139
Received 1991 September 6; accepted 1991 November 8

ABSTRACT

We attempt to measure rotational broadening of absorption lines in a sample of 47 nearby, late K- and M-type main-sequence stars. For each star, we measure $v \sin i$ from four lines by fitting them with artificially broadened lines from an extremely slowly rotating reference star of similar spectral type. We compare this convolution technique to a proper disk integration of specific-intensity line profiles and show that the derived $v \sin i$ values agree to within 0.5 km s^{-1}. Rotation is detected above a threshold of 3 km s^{-1} in five stars: AD Leo, EQ Vir, YZ CMi, Gliese 369, and Gliese 569. The known rotation period for AD Leo permits an estimate of its inclination, $33° < i < 44°$, and thus the polar region of one hemisphere is always in view. A similar analysis for EQ Vir yields a mutually consistent rotation period and $v \sin i$, implying an aspect nearly equator-on. The presence of detectable rotation for GL 569A confirms that the system is indeed younger than about 1 Gyr. Thus its low luminosity companion remains an outstanding brown dwarf candidate. Upper limits for $v \sin i$ of 2–3 km s^{-1} are derived for the nondetections, all magnetically inactive M dwarfs. The average equatorial rotational velocity of M dwarfs in the solar neighborhood is less than 2 km s^{-1}. This confirms M dwarfs as the slowest rotators on the main sequence and suggests that many lose about 98% of their angular momentum during their main sequence lifetimes. Zeeman broadening is shown to be negligible in optical lines of inactive M dwarfs.

Subject headings: stars: late-type — stars: rotation

1. INTRODUCTION

The rotation of main-sequence stars has been carefully studied for all spectral types except for the M-type stars. Even for the slowly rotating G- and K-type dwarfs, good measurements have been derived via both rotational Doppler broadening of absorption lines and periodicities in the brightness of chromospheric lines (cf. Noyes et al. 1984; Soderblom 1985). But for M dwarfs, even the detection of rotation has been hampered by both their intrinsic faintness and their exceedingly slow rotation, typically less than 10 km s^{-1} at the equator (Stauffer & Hartmann 1986). An exception has emerged for the very young M dwarfs in clusters, with rotation measurements made possible by their surprisingly high spin rates (cf. Hartmann & Stauffer 1989; Stauffer et al. 1991; Prosser, Stauffer, & Kraft 1991). These measurements have led to an improved theoretical understanding of the angular momentum history of low-mass stars (Kawaler 1989; Pinsonneault, Kawaler, & Demarque 1990).

The rotation of M dwarfs bears on several astrophysical issues. Chromospheric emission lines and surface "starspots" apparently occur only in M dwarfs rotating above a threshold equatorial velocity of about 5 km s^{-1} (Bopp & Fekel 1977; Bopp & Espanek 1977; Vogt, Soderblom, & Penrod 1983, hereafter VSP; Byrne, Doyle, & Menzies 1985; Pettersen 1989). However, little is understood about the dynamo generation of the magnetic fields that presumably cause this surface activity. Also mysterious is the physics underlying the rotational history of low-mass stars. At ages of about 5 Myr (seen as low-mass T Tauri stars), their equatorial velocities are about 15 km s^{-1} (Hartmann et al. 1986), three orders of magnitude lower than predictions based on the specific angular momentum of protostellar clouds. At ages of about 50 Myr, about half of the M dwarfs exhibit equatorial velocities of 50–100 km s^{-1}. While this may be explained by a prior decrease in their moment of inertia (Stauffer 1991), it is not understood why only half are spinning rapidly. At ages of 500 Myr, as seen in the Hyades, the most rapidly rotating M dwarfs have rotational velocities of 15–20 km s^{-1}. But most M dwarfs in the Hyades have rotational velocities less than 10 km s^{-1} (Radick & Baliunas 1987; Stauffer, Hartmann, & Latham 1987; Stauffer et al. 1991). It is not known whether the entire interior of the M dwarf has decelerated or just the envelope, though this issue may have little consequence. During their main-sequence lifetimes, M dwarfs apparently continue to lose angular momentum by processes not entirely understood, but which are presumably related to a wind. But the average rotation of a middle-aged M dwarf is not known because very few have been monitored long enough to reveal chromospheric or photometric modulations.

Here, high-resolution spectra of a sample of 47 dwarfs in the solar neighborhood are analyzed for rotational broadening. The sample includes dwarfs from K5 to M5, here loosely termed "M dwarfs," as a shorthand. It is expected that most will not exhibit detectable rotation, so our intention is to establish stringent upper limits for those cases. For the detections, we establish a $v \sin i$ analysis that maintains high precision for spectra of high-resolution and modest signal-to-noise (S/N) ratio.

[1] On leave from San Francisco State University. Postal address: Department of Physics and Astronomy, San Francisco State University, San Francisco, CA 94132.

2. OBSERVATIONS

The sample of M dwarfs was selected from Joy & Abt (1974) with the criteria that they be single (to avoid spectroscopic confusion) and bright enough ($V < 11$) for high-resolution spectroscopy. The sample may contain a slight bias against stars of extremely low space velocity, since the M dwarfs in Joy & Abt were primarily detected by proper motion. However, all sample stars lie within 20 pc, a distance within which even very small space velocities yield detectable proper motion (Gliese, Jahreiss, & Upgren 1987). The spectra were originally obtained for another purpose, namely to detect extremely low mass companions to M dwarfs via Doppler shift measurements (Marcy, Lindsay, & Wilson 1987; Marcy & Benitz 1989).

The spectra were acquired with the Lick Observatory echelle "Hamilton" spectrograph (Vogt 1988) and TI CCD, yielding a resolution of 40,000 and covering from 5000 to 8000 Å with gaps between spectral orders. The reduction of the raw CCD images was standard and was described in detail previously (Marcy, et al. 1987). The sample M dwarfs have V magnitudes of 8–11, which in exposures of 5–30 minutes yielded a signal-to-noise ratio of typically 30. For the present study, only four spectral orders were used, each about 40 Å long centered on $\lambda\lambda$6130, 6070, 5710, 5595. Most observations were made with a slit width of 330 μm (=0".6), but a few were made with a slit of 500 μm and thus had a lower resolution of only 30,000.

3. ROTATION ANALYSIS

3.1. *Overview of Techniques*

Rotational broadening can be measured by several techniques for line-rich spectra such as these. The cross-correlation function width (e.g., Tonry & Davis 1979; Latham 1985) has been used extensively for spectra of modest S/N ratio with great success. The large sections of the spectrum used in this technique proved to be a disadvantage here owing to the inclusion of molecular band heads and associated molecular features which tend to exhibit great temperature sensitivity, thus causing significant biases in the derived rotational velocities. Mismatches in spectral type as small as one subclass between the template and program star led to systematic errors of 1 km s^{-1} in rotation velocity, owing primarily to molecular features. Similar errors are incurred by Fourier-Quotient techniques which additionally require filtering of high-frequency noise.

Rotation analysis by line-transfer synthesis of individual lines represents the most straightforward method for determining v sin i. However, it is possible only if reliable model atmospheres exist, which is not the case for M dwarfs where molecular opacities are poorly known. This approach was adopted by VSP who used M dwarf atmospheres from Mould (1976) and an assumed macroturbulent velocity of 3 km s^{-1} throughout. The Mould atmospheres suffer from inadequate molecular opacity data, and the assumption of a constant macroturbulent velocity probably introduces errors in the derived rotational velocities of about 1 km s^{-1}.

We choose to measure rotational velocities by fitting individual lines with a rotationally broadened spectrum of a nonrotating M dwarf star (Gray 1976). This approach carries three advantages:

1. We may restrict the analysis to atomic lines having low temperature sensitivity.

2. We automatically include macroturbulence in the nonrotating reference star of similar spectral type.

3. Blends in the line wings are automatically included in the rotationally broadened nonrotating template. The assumption is made here that stars of similar spectral type have nearly the same macroturbulence.

This assumption is entirely untested for M dwarfs, but we will show in § 3.2 that the range of macroturbulent velocities represented by M dwarfs is certainly less than 2 km s^{-1}. We also assume that the convolution of the rotational broadening function with a stellar flux spectrum adequately synthesizes the spectrum from a rotating star. We test this hypothesis in § 3.5.

3.2. *Nonrotating Reference M Dwarfs*

The analysis requires use of the spectrum of an M dwarf that has an equatorial velocity so low that the other line-broadening mechanisms, namely, thermal Doppler, microturbulence, macroturbulence, collisional broadening, and curve-of-growth effects, dominate the line profile. There are no established standard stars for rotational velocity among the M dwarfs, but there are several that are almost certainly rotating with $v_{eq} < 2$ km s^{-1}. Among the stars in our sample, we identified two, GL 411 (=HD 95735, dM2) and GL 820B (=61 Cyg B, dM0/dK7) as having absorption lines among the narrowest observed. Confirmation of their suitability as "nonrotating" stars comes from observed periodicities in their Ca II H and K emission. The observed rotation periods are 48 days, coincidentally, for both stars (Vaughan et al. 1981; Baliunas et al. 1983; Noyes et al. 1984). Such long periods coupled with stellar radii of about 0.5 $R_\odot$ ensure that $v_{eq} < 1$ km s^{-1} in both cases. We note that GL 411 has old disk space motions and photometric characteristics (Stauffer & Hartmann 1986), and IR spectroscopy shows it to be metal-poor (Mould 1978). We adopt the spectra of these two stars as the templates to be rotationally broadened for comparison with the other program stars.

These two "nonrotating" standards have different spectral types and metallicities which may cause differences in line widths unrelated to rotation. We carefully explored these effects by fitting Gaussians to four neutral metal lines, namely λ6126.2, λ6141.7, λ6085.3, and λ5703.5, and measuring their Gaussian widths and equivalent widths, W_{eq}. We calibrated the Gaussian widths in terms of rough measurements of rotation, i.e., v sin i, by applying via convolution, the rotational broadening function to one spectrum of GL 411 and measuring the Gaussian widths as a function of applied v sin i. We then measured the Gaussian widths of the same four lines in the spectra of all program stars, thus obtaining a measure of the line-broadening relative to the lines in GL 411. This measure of line broadening represents some physically ill-defined enhancement of line widths, as if due entirely to rotational broadening relative to those in GL 411. The average value for the four lines was taken to be this pseudorotational line broadening for each star.

In Figure 1, we show these measurements of line broadening plotted against the mean equivalent width of the four lines. Several stars are identified by their Gliese numbers on the plot, and, as expected, GL 411 and GL 820B lie near the bottom of the scatter. (Note that GL 411 does not sit exactly at zero because this point is the average of two observations, while the template was taken to be the higher quality of the two.) Significantly, Figure 1 exhibits a trend such that stars having larger W_{eq} tend to have greater line broadening. This trend demonstrates that some enhancement in line width is caused by

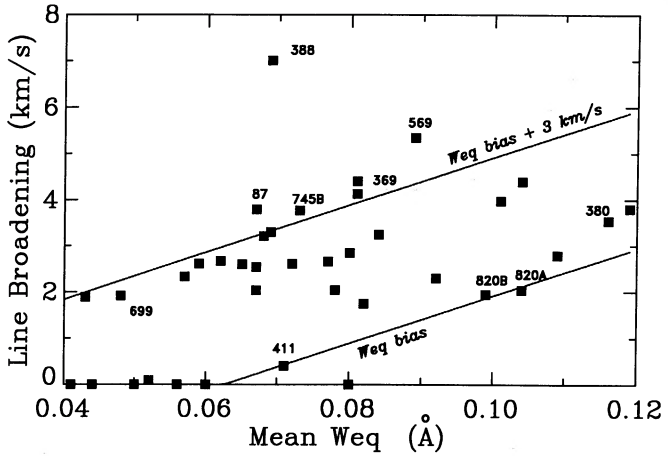

FIG. 1.—Excess line broadening of M dwarfs vs. the mean equivalent width of four metal lines. The excess broadening is relative to the "nonrotating" standard, Gliese 411, and has been interpreted as entirely due to rotation, which is clearly not the case. The apparent trend in the lower envelope, sketched as "W_{eq} bias," shows that line width also depends on equivalent width and affects v sin i measurements by as much as 3 km s^{-1}.

metallicity and spectral-type differences between the program stars and GL 411 and is not due to rotation alone. The lower envelope of the points, shown as a dashed line labeled "W_{eq} bias," passes through GL 411 and GL 820B, both known to exhibit essentially no rotational broadening, as discussed above. This lower envelope rises about 3 km s^{-1} from the lowest observed W_{eq} to the highest. Thus the trend seen in Figure 1 shows that the details of the line transfer, including metallicity and atmospheric characteristics, will introduce errors in measurements of v sin i of about 3 km s^{-1}.

We have attempted to suppress this error in v sin i by segregating the program stars and the two template stars according to the mean W_{eq} of the four metal lines. We therefore designated GL 820B ($\langle W_{eq} \rangle = 99$ mÅ) as the template for all stars having $\langle W_{eq} \rangle$ greater than 85 mÅ, and GL 411 ($\langle W_{eq} \rangle = 66$ mÅ) for all stars having $\langle W_{eq} \rangle$ less than 85 mÅ. It is apparent, however, that these two templates represent only two points on a continuum of nonrotational enhancement of line width that spans 3 km s^{-1} along the W_{eq}-bias line in Figure 1. We thus expect that use of these two templates in their respective regimes may still permit errors in the determination of v sin i of as much as 2 km s^{-1} owing to line broadening that is unaccounted for.

3.3. *The Rotation Technique*

The actual measurement of rotational broadening, v sin i, for all program stars was determined by fitting the four neutral metal lines (listed in § 3.2) with the same lines in the appropriate template that has been synthetically broadened by the rotational broadening function (Gray 1976). We adopted a limb-darkening coefficient of 0.6, and trials with a coefficient of 0.3 yielded changes in the derived v sin i of only 0.1 km s^{-1}, insignificant here. The fitting was done by first scaling the line profile depths of the template to that of the program star. The linear scaling was done by simply multiplying the line depth at each wavelength across the profile to force equal equivalent widths of the star and template. The amount of scaling required was always less than 30% and usually less than 10% because of the appropriate choice of template, described above.

The analysis involved generating broadened templates for values of v sin i from 0 to 10 km s^{-1} in steps of 2 km s^{-1}. The quality of the fits was characterized by a χ^2 statistic for each v sin i, and the "best-fit" v sin i was determined by a parabolic fit to the χ^2 function to locate its minimum. These values of v sin i for each of the four lines were averaged, weighted by the inverse of χ^2, to yield the final determination of v sin i for a given observation. We also computed the weighted uncertainty in the mean of the four values of v sin i which gives an estimate of the internal error in the final v sin i. The final measurements of v sin i are listed in Table 1.

Columns (1) and (2) in Table 1 give the Gliese numbers of the program star and the reference template, respectively, and column (3) states whether the spectrum was of high or low resolution. Column (4) gives the average W_{eq} of the four metal lines used in the analysis. Columns (5)–(8) give the value of v sin i derived for each of the four lines, and columns (9) and (10) give the final weighted average and uncertainty of the mean in v sin i.

For several stars, a slightly modified procedure was adopted. For Gliese 15B, 273, and 285, the spectra had an extraordinarily low S/N ratio of between 10 and 20. For these poor cases, the narrow lines used for all other stars were difficult to isolate, and so four stronger lines were used, namely, λλ5588.8, 5594.5, 5601.3, and 5602.8, all low-excitation lines due to Ca I. These lines have stronger wings and are more "saturated" than the four standard lines used here, and so carry less sensitivity to rotational broadening. This diminished sensitivity and the low S/N are reflected in the greater scatter in the measured values of v sin i for the four lines. The uncertainties in the mean v sin i are all above 2 km s^{-1}, the worst of all the program stars. Nonetheless we felt it useful to provide v sin i measurements of lower quality rather than reject the spectra entirely. The spectrum of GL 908 had sufficiently poor quality that we analyzed it both with the usual four lines and with the four strong Ca I lines, giving 3.1 and 1.8 km s^{-1}, respectively.

For GL 517 (=EQ Vir) a different grating setting was used, as a part of a different project, resulting in loss of two lines, namely, λλ6141 and 6085. Therefore, we replaced them with two other neutral metal lines, λ6119.5 and λ5590.1. This star has such a large v sin i, 8.3 km s^{-1}, that line broadening is dominated by rotation, and indeed the two new lines gave essentially the same value as the standard two lines (see Table 1). For GL 517 we also chose to use GL 820A (61 Cyg A) instead of GL 820B (61 Cyg B) as the template because of the good match between the two in spectral type, K5 Ve and K5 V. (Using GL 820B as the template for the analysis of GL 517 yielded a value of v sin i 0.4 km s^{-1} greater than that using GL 820A as template.) Note that the magnetic activity of emission-line, active stars such as EQ Vir (Saar 1987) may result in different atmospheric characteristics. We discuss in § 4.3 the possibility that Zeeman broadening contributes to the line broadening (Benz & Major 1984).

We adopted the following criteria for a definitive detection of rotational broadening:

1. The derived value of v sin i must exceed 3 km s^{-1} (averaged over all observations).
2. The derived v sin i must exceed twice the derived uncertainty.

Table 1 shows that only five of the 47 stars yielded a measured value of v sin i that meets both criteria for definitive detection. These five detections of v sin i are GL 285 (YZ CMi), GL 369,

TABLE 1

ROTATIONAL VELOCITIES OF ALL PROGRAM STARS

STAR (Gliese number) (1)	REFERENCE TEMPLATE (Gliese number) (2)	RESOLUTION (3)	$\langle W_{eq} \rangle$ (mÅ) (4)	$V \sin i$ (km s^{-1}) λ6126 (5)	λ6141 (6)	λ6085 (7)	λ5703 (8)	$\langle V \sin i \rangle$ (km s^{-1}) (9)	UNCERTAINTY (km s^{-1}) (10)
14	820B	Low	111	2.9	2.8	3.0	1.5	2.6	0.3
15B	411	Low	100	8.4	9.9	0.0	7.2	<8.0[a]	2.3
26	411	Low	64	0.0	4.3	0.0	2.5	2.9	1.1
87	411	Low	70	1.0	0.4	0.8	9.9	1.1	1.1
87	411	High	67	3.1	4.4	1.5	4.3	3.1	0.7
273	411	High	50	0.0	4.6	0.0	8.1	3.4[a]	2.1
285	411	High	60	9.9	0.8	2.1	2.8	4.8[a]	2.3
369	411	High	81	0.4	3.2	8.7	2.9	4.8	1.5
380	820B	High	118	4.0	1.2	1.9	0.0	2.1	0.8
380	820B	High	114	3.0	1.8	2.8	0.3	1.7	0.5
388	411	High	60	6.3	5.5	9.9	4.9	6.5	1.0
388	411	High	78	4.6	5.8	7.4	4.7	5.6	0.5
393	411	High	41	1.2	0.1	0.0	0.0	0.1	0.2
411	411	Low	60	0.0	0.0	0.0	0.0	0.0[b]	0.0
411	411	High	71	0.0	0.0	0.0	0.0	0.0[b]	0.0
412A	411	High	100	1.1	2.1	1.9	1.0	1.6	0.3
414A	820B	High	119	1.9	2.2	4.1	0.8	2.7	0.7
414B	820B	High	90	7.3	0.0	3.7	0.2	3.2	1.9
436	411	High	80	2.5	0.4	5.7	0.0	1.0	0.9
459.3	820B	High	104	1.6	1.3	3.1	3.2	2.8	0.4
461	820B	High	101	3.4	3.3	3.2	0.0	2.5	0.8
464	411	High	81	0.0	0.9	2.9	2.6	2.4	0.5
480	411	High	61	0.0	0.0	0.0	0.0	0.0	0.0
480	411	High	58	0.0	0.0	2.0	0.8	0.6	0.3
507.1	411	Low	50	9.9	1.8	0.0	1.4	2.6	1.7
507.1	411	High	59	1.1	2.7	2.8	4.0	2.8	0.3
517	820A	High	110	7.8	9.3	9.0	6.9	8.3[c]	0.5
521	411	Low	51	3.6	0.0	0.0	2.7	2.0	1.0
526	411	Low	63	2.6	0.0	0.3	6.6	1.0	0.9
526	411	High	80	4.3	2.5	3.4	1.7	2.6	0.4
552	411	High	59	5.6	0.2	9.9	0.1	1.2	1.2
552	411	High	77	0.0	0.0	1.3	0.3	0.3	0.3
569	411	High	83	4.2	3.2	5.5	3.1	4.0	0.6
569	820B	High	95	5.1	2.3	4.8	1.6	2.9	0.8
570.2	411	High	71	0.0	4.4	0.0	2.7	2.5	1.1
570.2	411	High	82	3.3	2.6	0.9	3.8	2.9	0.6
570B	411	High	81	3.4	1.6	4.0	4.0	2.9	0.6
570B	411	High	76	3.1	3.0	1.6	1.0	2.2	0.5
581	411	High	42	0.0	0.0	0.4	1.3	0.4	0.3
581	411	High	46	3.4	0.0	0.0	0.0	0.1	0.3
623	411	High	47	0.0	0.5	2.0	0.8	0.6	0.4
623	411	High	45	2.2	1.2	0.0	0.0	1.1	0.5
623	411	High	65	2.9	0.0	1.6	1.3	1.3	0.6
638	820B	High	101	1.3	2.7	0.8	0.0	1.4	0.5
638	820B	High	117	2.5	2.3	0.7	0.0	1.6	0.6
649	411	High	73	1.5	2.4	0.0	2.1	1.9	0.4
649	820B	High	91	3.1	0.0	0.0	0.0	0.8	0.8
654	411	High	70	3.8	0.0	2.4	1.6	1.1	0.8
694	411	High	52	0.8	1.8	0.9	0.0	1.4	0.3
694	411	High	60	0.0	4.6	1.2	0.0	2.8	1.2
699	411	Low	43	9.9	3.0	6.8	0.0	5.4	1.8
699	411	High	42	0.0	4.9	2.8	0.0	2.5	1.3
699	411	High	54	0.0	2.6	9.9	0.0	2.0	1.5
701	820B	High	85	0.0	0.7	2.8	0.0	0.8	0.5
720A	411	High	83	2.1	3.7	0.1	0.0	1.5	0.9
720A	820B	High	101	0.1	0.6	1.0	0.0	0.4	0.2
745A	411	High	65	4.0	2.5	0.0	1.3	2.6	0.6
745A	411	High	79	9.9	3.8	3.5	1.4	3.5	1.0
745B	411	High	71	5.0	3.7	0.0	1.5	3.0	0.9
745B	411	High	75	3.6	0.0	4.7	0.0	1.2	1.1
748	411	High	47	4.8	5.1	7.4	0.0	4.6	1.3
748	411	High	38	1.7	1.7	5.8	1.0	2.0	0.8
752A	411	High	66	4.0	0.0	4.3	0.0	0.8	1.0
806	411	High	67	0.0	3.6	1.0	0.0	1.5	0.8
806	411	High	67	8.2	1.5	3.6	2.2	3.7	1.6
820A	820B	High	104	0.4	0.8	0.9	0.9	0.7	0.1
820A	820B	High	104	0.0	2.4	0.0	0.0	0.8	0.6

TABLE 1—*Continued*

Star (Gliese number) (1)	Reference Template (Gliese number) (2)	Resolution (3)	$\langle W_{eq} \rangle$ (mÅ) (4)	$V \sin i$ (km s^{-1}) λ6126 (5)	λ6141 (6)	λ6085 (7)	λ5703 (8)	$\langle V \sin i \rangle$ (km s^{-1}) (9)	Uncertainty (km s^{-1}) (10)
820B	820B	High	101	0.0	0.0	0.0	0.0	0.0[b]	0.0
820B	820B	High	104	2.5	0.5	0.0	0.0	0.7	0.5
820B	820B	High	92	0.4	1.0	0.7	0.0	0.5	0.2
849	411	Low	43	0.0	0.2	2.0	3.1	1.0	0.6
851	411	Low	69	1.7	3.7	1.5	3.6	2.5	0.6
851	411	High	57	0.0	2.7	3.4	0.1	2.1	0.9
863	411	High	69	4.1	0.6	0.9	0.0	1.8	1.0
876	411	Low	33	4.9	0.3	9.9	0.0	2.8	2.2
880	820B	Low	88	0.0	0.0	3.1	6.0	1.1	1.1
908	411	Low	69	2.9	4.7	0.7	2.3	3.1[d]	0.9

[a] Low S/N: used λλ5588.8, 5594.5, 5601.3, 5602.8 which are deeper and intrinsically broader, hence less sensitive to $V \sin i$.
[b] Test case: Star was used as its own reference.
[c] Used lines λλ6119.5, 6126.2, 5703.5, 5590.1 due to different grating tilt.
[d] Using lines in footnote a, we obtained $v \sin i = 1.8 \pm 0.7$.

GL 388 (AD Leo), GL 517 (EQ Vir), and GL 569, the derived values for which are listed in Table 2.

For the remaining 42 stars, the measured values of $v \sin i$, though listed in Table 1, must be considered dubious at best and better interpreted as upper limits. The detectability threshold of 3 km s^{-1} represents the most prudent upper limit, as we now discuss.

3.4. *Errors and Thresholds for Detection of* $v \sin i$

Errors in the derived $v \sin i$ measurements come from several sources. Those due to photon statistics are certainly represented by the uncertainty in the mean $v \sin i$ of the four lines as given in the last column of Table 1. Similarly any random errors caused by, for example, bad pixels on the CCD, cosmic-ray hits, or occasional poor flat-fielding, will show up as deviations in the derived $v \sin i$ values for the four lines of a given observation. The last column of Table 1 shows that the accumulation of these random errors amounts to about 1 km s^{-1} typically. Many stars were observed more than once, and in every case the measured values of $v \sin i$ agree within ± 2 km s^{-1} of the average, and usually within 1 km s^{-1}. This result confirms that random errors are about 1 km s^{-1}.

More serious are the systematic errors due to mismatch between template and program star. Differences must exist in both the line transfer (because of different atmospheric structures and metallicities) and turbulence characteristics among stars from dM0 and dM5, producing some differential line broadening that masquerades as rotation. As discussed in § 3.2 and shown in Figure 1, the "W_{eq}-bias" suggests that differential line broadening of unspecified origin depends in part on average W_{eq} and has a magnitude of about 2 km s^{-1} relative to the appropriately chosen template stars. Thus, empirically, the systematic errors in $v \sin i$ due to spectral mismatching may be as much as 2 km s^{-1}. Assuming M dwarfs are as homogeneous as G and K dwarfs in surface turbulence (Soderblom 1983; Benz & Mayor 1984), it is likely that the macroturbulent velocities vary by less than 2 km s^{-1} over such a narrow range in spectral type. Indeed, VSP adopted a constant macroturbulence of 3 km s^{-1} for all K and M dwarfs in their rotation

TABLE 2

$v \sin i$ Detections and Comparison with Other Measurements

Gliese Number (1)	Other Name (2)	Number of Observations (3)	$v \sin i$ (km s^{-1}) (4)	Uncertainty (km s^{-1}) (5)	Other $v \sin i$ (km s^{-1}) (6)	P_{rot} (days) (7)
285	YZ CMi	1	4.8[a]	2.3	...	2.8[b]
369	...	1	4.8	1.5	...	...
388	AD Leo	2	5.8	0.5	5.0[c]	2.7[d]
517	EQ Vir	1	8.3	0.5	9.9[e]	3.96[f]
569	...	2	3.6	0.6	...	...
638	HD 151288	2	<2	0.6	<3	...
820A	61 Cyg A	2	<2	0.6	<1[g]	38[h]
880	HD 216899	1	<2	1.1	<3	...

[a] Poor spectrum: S/N ≈ 20.
[b] Chugainov 1974.
[c] Vogt, Soderblom, & Penrod 1983.
[d] Spiesman & Hawley 1986.
[e] Saar, Linsky, & Beckers 1986; also, Saar (9.25 km s^{-1}; 1991, private communication), VSP (10.8 km s^{-1}).
[f] Ferraz Mello & Torres 1971.
[g] Benz & Mayor 1984.
[h] Baliunas et al. 1983.

analysis. In summary, spectral mismatches may result in systematic errors of 2 km s^{-1} and random errors are about 1 km s^{-1}. We thus find 3 km s^{-1} to be the detection threshold for the present effort. Measured values between 2 and 3 km s^{-1} indicate the possible *presence* of real rotational broadening especially in cases of small uncertainty, but no quantitative estimate of $v \sin i$ is possible for them.

We note that errors in a $v \sin i$ measurement can also be caused by peculiarities in the object itself. Most notably, unresolved spectroscopic binaries may exhibit broad lines simply due to the composite spectrum. In principle, this can be checked photometrically, since the combined magnitude should be greater than that expected for a single star. Also, equatorial starspots covering a significant portion of the limb of the disk will "remove" rotational line broadening.

3.5. *Test of Convolution versus Disk Integration*

The technique employed here assumes that the convolution of the rotational broadening function with the flux spectrum from a nonrotating star adequately reproduces the actual spectrum from a rotating star. We tested this assumption by generating LTE *specific intensity* line profiles for eight values of $\cos \theta$ over the hemisphere of a hypothetical late-type star. A disk integration of these profiles was carried out, employing 1200 grid points over the stellar surface. We tried cases for an equatorial rotation of 0, 2, 4, 6, 8, and 10 km s^{-1} in the disk integration, and included radial-tangential macroturbulence of 3 km s^{-1} to make the resulting flux profiles as realistic as possible. The case having zero rotation represents the observed flux spectrum from a nonrotating star, such as those used in the convolution technique here.

We convolved this zero-rotation flux profile with the rotational broadening function for 2, 4, 6, 8, and 10 km s^{-1} and compared the resulting convolved profiles with those generated properly with disk integration. In each case, the comparison showed differences of about 0.5% of the continuum level. *Therefore, we find that convolution by the rotational broadening function reproduces disk-integrated flux profiles with a precision of* 0.5%. No fitting was done here, and thus we find that the values of $v \sin i$ derived by convolution techniques correspond directly to the actual value of $v \sin i$. (This is not the case for determinations of macroturbulence for which convolution and disk integration yield different model-dependent values.)

As an example, Figure 2 shows a flux profile generated by disk integration for $v \sin i = 7$ km s^{-1}, overlaid on flux profiles generated by convolution for $v \sin i = 4$, 6, 8, and 10 km s^{-1}. The figure shows that the points (*squares*) of the disk-integrated profile for 7 km s^{-1} lie entirely between the convolution profiles for 6 and 8 km s^{-1}. *This shows that an error of less than* 0.5 km s^{-1} *is made by using convolution to fit observed (disk-integrated) profiles, independent of their S/N ratio.* However, for spectroscopic analyses in which the quality of the fit is paramount and for which the spectra have S/N > 100, disk integration may be required.

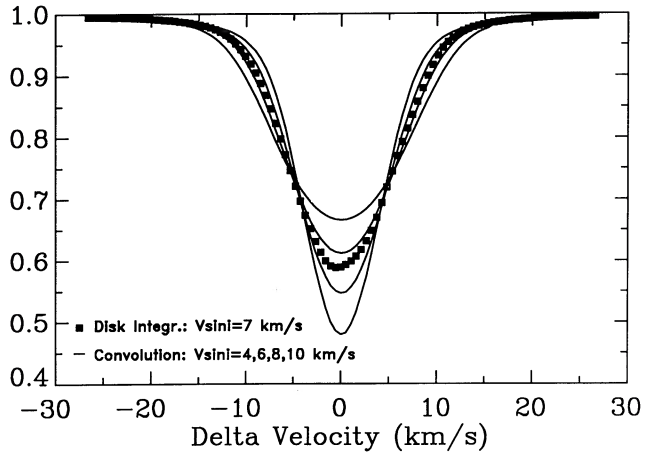

FIG. 2.—A rotationally broadened, theoretical flux profile, for $v \sin i = 7$ km s^{-1} (*squares*), overlaid on profiles constructed by disk integration for different assumed $v \sin i$. The rotationally broadened profile for 7 km s^{-1} lies between the disk-integrated profiles for 6 and 8 km s^{-1}. Thus, convolution with the rotational broadening function preserves precision of $v \sin i$ to within 0.5 km s^{-1}.

4. DISCUSSION

4.1. *Rotation of Individual Stars*

The present rotation analysis of M dwarfs is similar to that of Vogt & Fekel (1979) and Pettersen et al. (1987) in that we compare observed absorption line profiles to artificially rotationally broadened profiles of an extremely slowly standard star of nearly the same spectral type. The high resolution of the present spectra permit detection of rotational broadening above 3 km s^{-1} and yield uncertainties in $v \sin i$ similar to those of VSP, albeit by a different analysis. Figure 3 shows the line profile fits for some representative cases, both detections and nondetections of rotational broadening. In each case, the observed profile is overplotted on a set of template profiles broadened by trial amounts of 0, 5, 10, and 15 km s^{-1}, for comparison. The cases of EQ Vir and AD Leo (Gliese 517 and 388) show clear evidence of rotational broadening. The examples in Figure 3 of nondetections of rotational broadening, GL 623 and GL 380, show profiles that are consistent with no more than 3 km s^{-1} for $v \sin i$, the threshold for definitive detection.

Among the 47 stars observed here, only five exhibited detectable rotational broadening, as discussed in § 3.3. The results for these five detections are listed in Table 2. Columns (1) and (2) give the Gliese number and alternative name, and column (3) gives the number of observations for each. Column (4) gives the average velocity from all observations, weighted by the inverse square of the uncertainty given in Table 1, and column (5) gives the lowest uncertainty of the original observations. Column (6) lists previous measurements of $v \sin i$ by other investigators and column (7) gives the rotation period as determined by spectroscopic or photometric periodicities, with the origins given in the footnotes.

Also listed in Table 2 are the three stars, GL 638, GL 820A, and GL 880, that have a previous measurement of $v \sin i$, all nondetections here. These three similarly exhibited no measurable rotation in the survey by VSP, providing similar limits to $v \sin i$. We have listed the upper limits to $v \sin i$ for these stars as 2 km s^{-1} despite our general threshold for detection of 3 km s^{-1} because in these three cases the measured values of $v \sin i$ are each less than 2 km s^{-1}. Thus, it is unlikely that the actual $v \sin i$ is as high as 2 km s^{-1} for any of the three. For these stars, we listed an uncertainty equal to the highest uncertainty of any of the individual observations, all of which are less than 1.1 km s^{-1}.

The two stars having previous nonzero $v \sin i$ measurements, namely GL 388 (AD Leo) and GL 517 (EQ Vir), permit com-

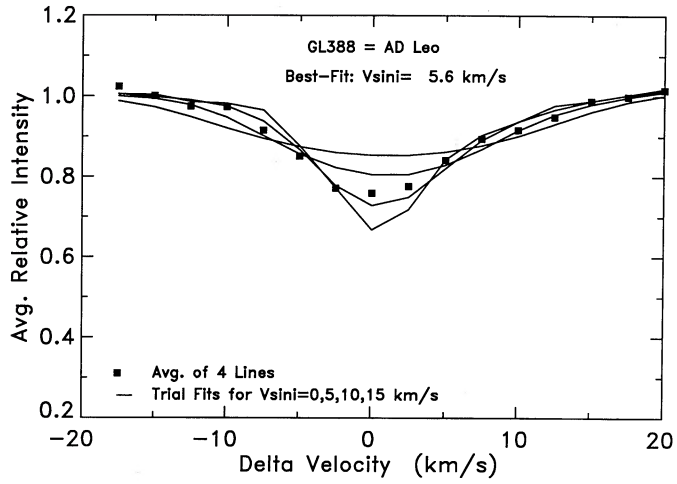

FIG. 3a

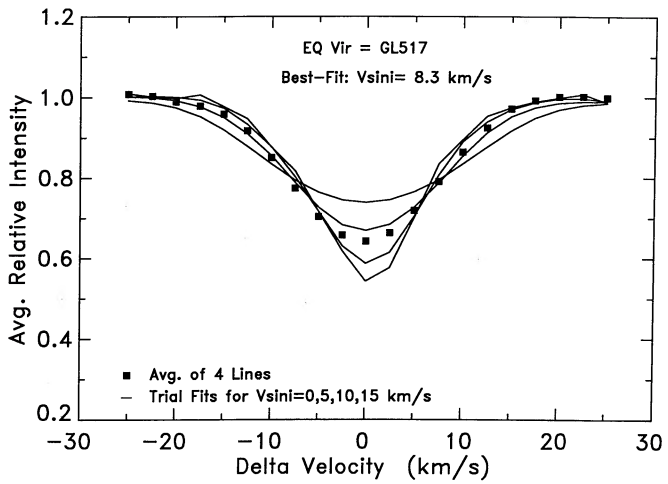

FIG. 3b

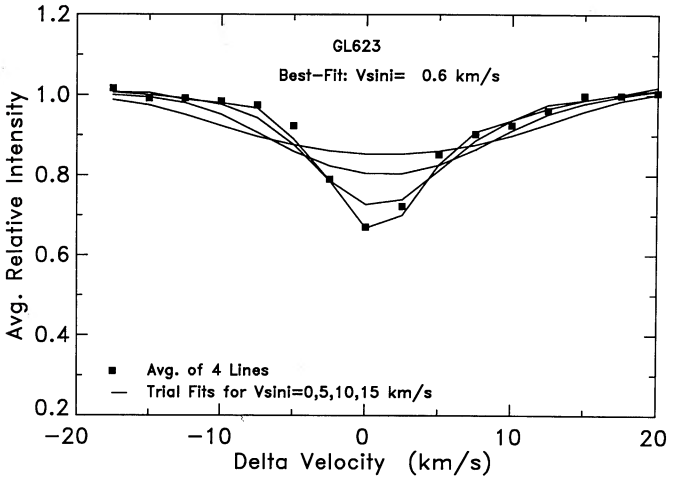

FIG. 3c

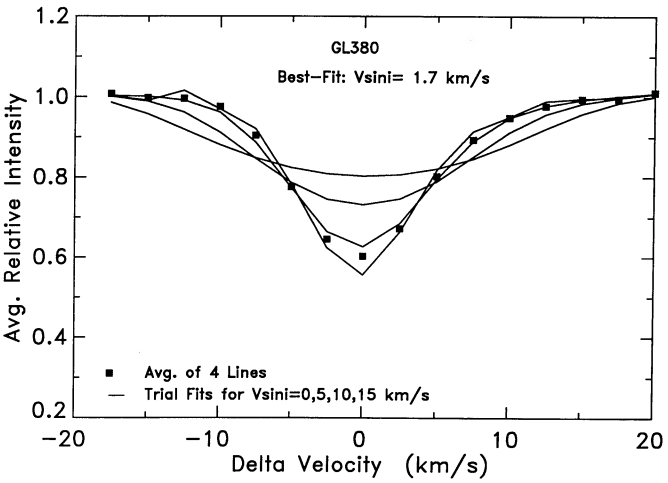

FIG. 3d

FIG. 3.—The average of four observed line profiles (*squares*) plotted over synthetic profiles for different trial values of v sin i. Figs. 3*a* and 3*b* show AD Leo and EQ Vir, representative of detected rotation. Figs. 3*c* and 3*d* show Gliese 623 and 380, representative of nondetections.

parison with other v sin i efforts. Our v sin i for AD Leo agrees with that from VSP (5.8 and 5.0 km s^{-1}, respectively). Our value of v sin i for EQ Vir (8.3 km s^{-1}) agrees modestly with two recent measurements. Saar, Linsky, & Beckers (1986) found 9.9 km s^{-1} and later, S. H. Saar (private communication 1991) obtained 9.25 km s^{-1}. However, VSP obtained 10.8 km s^{-1}. The following contains a compilation of quantities related to rotation for each interesting star.

EQ Virginis.—One may directly compute the rotation velocity at the equator from the rotation period, for subsequent comparison with the v sin i measurements. The stellar radius can be derived from Lacy's (1977) empirical relations, giving $R/R_\odot = 0.68$ for dK5, in agreement with Pettersen (1989) who gives $R/R_\odot = 0.74$. We adopt the average radius of 0.71 $R_\odot$ with an uncertainty of 0.1 $R_\odot$, based on the scatter in Lacy's calibration. This radius, combined with the rotation period, $P_{\rm rot} = 3.96$ days (Ferraz Mello & Torres 1971), gives an equatorial velocity of $V_{\rm eq} = 9.0 \pm 1.2$ km s^{-1}, identical to Pettersen's (1989) value, 9 km s^{-1}, which was computed similarly. This equatorial velocity is consistent with (i.e., higher than) the measured v sin i here of 8.3 km s^{-1}. The inclination, i, is inferred to be 67°, with an uncertainty range of $-12°/+23°$, estimated by adding linearly the fractional uncertainty in radius to the internal uncertainty in v sin i.

The fit of EQ Vir by its rotationally broadened template 61 Cyg A, is good as indicated in Figure 3, implying minimal errors in this determination of v sin i. The fit is certainly aided by the apparently good spectral type match between EQ Vir (dK5e) and 61 Cyg A (dK5), thereby minimizing the errors due to different atmospheric and turbulent characteristics. The small uncertainty in the mean v sin i of the four measured lines, 0.5 km s^{-1}, reflects this good match. However, one cannot ignore the possibility that the spotted nature of EQ Vir causes a mismatch between it and 61 Cyg A, producing unrecognized errors in v sin i.

Two recent measurements of v sin i by Saar et al. (1986) and by S. H. Saar (1991, private communication) gave v sin $i = 9.9$ and 9.25 km s^{-1} respectively, consistent within errors of the v sin i here of 8.3 km s^{-1}. Saar's values are slightly larger than the equatorial velocity of 9.0 km s^{-1} derived from the rotation period, but the 15% uncertainty in the radius may account for this discrepancy. The v sin i by VSP of 10.8 km s^{-1} appears to

be slightly too high. In order for the equatorial velocity of EQ Vir to be as high as 10.8 km s^{-1}, either the radius of EQ Vir must actually be 0.85 $R_\odot$ (as they note), abnormally high for a K5 dwarf, or the rotation period must be 20% less than 3.97 days. VSP used only one line, λ6141 (Ba II), an analysis of which in our spectrum yielded $v \sin i = 9.3$ km s^{-1}, highest of four lines.

AD Leonis.—Our measured $v \sin i$ of 5.8 $\pm$ 0.5 (error in the mean $v \sin i$ of the four lines in our better measurement) agrees with VSP who find $v \sin i = 5.0 \pm 0.7$ km s^{-1}. The total error in our measurement is certainly no more than 2 km s^{-1} owing to possible differences between the reference star (GL 411, dM2) and AD Leo (dM3.5e). The uncertainty in the VSP measurement is probably similar due to poorly known macroturbulence and the approximate M-dwarf atmosphere used. Figure 3*a* shows trial fits to the line profiles from one observation of AD Leo, clearly exhibiting rotational broadening of between 5 and 7 km s^{-1}.

We determine the inclination of the rotation axis of AD Leo as follows. The rotation period of 2.7 days for AD Leo and two estimates of its radius, namely, 0.44 $R_\odot$ (Pettersen 1989) and 0.5 $R_\odot$ (Lacy 1977) yield equatorial velocities of 8.3 and 9.3 km s^{-1}, respectively. An estimate of the maximum possible inclination of the rotation axis is obtained from the ratio of the largest value of $v \sin i$, 5.8 km s^{-1}, to the smallest estimate of v_{eq}, 8.3 km s^{-1}. This gives $i < 44°$. Similarly, the minimum acceptable estimate of inclination is $i > 33°$. Thus, AD Leo is apparently viewed somewhat pole-on. Perhaps this small inclination is responsible for the long-standing difficulty in detecting broadband photometric periodicities due to spots (Bopp & Espanek 1977; VSP), especially if they reside preferentially near the poles.

Two sources of uncertainty in this inclination determination should be mentioned. First, the often-quoted rotation period of 2.7 days for AD Leo (Spiesman & Hawley 1986) requires confirmation, as the photometric information consists of only five nights of *BVRI* measurements spanning 11 days, with an apparent amplitude of only 3 times the photometric errors. Second, it is possible that the nearly equal $v \sin i$ values found by us and VSP are both systematically wrong by 1–2 km s^{-1} due to some unidentified effect. However, it is difficult to imagine a sufficiently gross error to account for the difference between the equatorial velocity of 8–9 km s^{-1} and the $v \sin i$ values of 5–6 km s^{-1}.

GL 569.—This dM2.5 star has an extremely low luminosity companion (GL 569B) which has an inferred mass near the H-burning limit (Forrest, Skrutsie, & Shure 1988; Henry & Kirkpatrick 1990). A mass determination requires knowledge of its age to place it on theoretical isochromes (cf. Burrows, Hubbard, & Lunine 1989). The detection of nonzero rotation here for GL 569A ($v \sin i = 3.6$ km s^{-1}) suggests that this system is young since almost all M dwarfs rotation more slowly. While no calibration exists between rotation and age for M dwarfs, we note that among the 74 stars surveyed here, GL 569A, ranks fifth highest in rotation. This implies that its age lies among the youngest 10% of field M dwarfs in the solar neighborhood.

We note that the average equivalent width of the four lines used in the $v \sin i$ analysis of GL 569A was close to the dividing line between the two templates, resulting in different templates being chosen for each of the two analyses. Nonetheless, the analyses of both spectra revealed rotation, 4.0 and 2.9 km s^{-1}, as indicated in Table 1. We consider the detection compelling but not convincing. If confirmed, the detection of rotation for GL 569 suggests unusual youth, probably less than 1 Gyr, based on rough calibrations of rotation by Raddick & Baliunas (1987), but not as young as the Pleiades. This suggestion of youth is consistent with other indicators of youth for the system, such as Hα emission and space motions (cf. Henry & Kirkpatrick 1991). Thus, GL 569B remains a credible brown dwarf candidate.

YZ Canis Minoris.—The present value of $v \sin i = 4.8 \pm 2.3$ should be used with caution given its large error. The rotation period of 2.77 days (Chugainov 1974; Pettersen et al. 1983) along with a radius from empirical relations yields an expected equatorial velocity of 5.6 km s^{-1} (Pettersen 1989), consistent with its $v \sin i$. No reliable estimate of inclination is possible because of the large uncertainty in $v \sin i$, but Pettersen (1983) finds that the dominating spot region is partly visible at all times.

4.2. *Rotation of Field M Dwarfs*

For each star in the survey, we computed the average $v \sin i$ from all observations, weighted by the inverse square of the uncertainty given in Table 1. Measurements below 3 km s^{-1} were taken at face value despite their proper interpretations as upper limits. Figure 4 contains a histogram showing the resulting $v \sin i$ measurements for all stars. The histogram shows that only eight of 47 stars exhibited $v \sin i$ above the detection threshold of 3 km s^{-1}, and three of those had uncertainties greater than half of the measurement causing doubt about those detections. Thus, only five of 47 showed definitive rotational broadening.

The histogram in the region $v \sin i < 3$ carries essentially no information both because it lies below the detection threshold as set by the error analysis in § 3.4 and because a bias exists which prevents measurements of $v \sin i$ less than zero. In the rotational analysis, values of $v \sin i$ less than zero cannot be tried in the profile fitting. Thus all sources of error are capable of producing spurious positive but not negative values of $v \sin i$. We therefore completely discount the peak and shape of the histogram seen for $v \sin i < 3$ km s^{-1}.

We now consider the average $v \sin i$ of late K-type and M dwarfs. The present sample of such field stars was selected

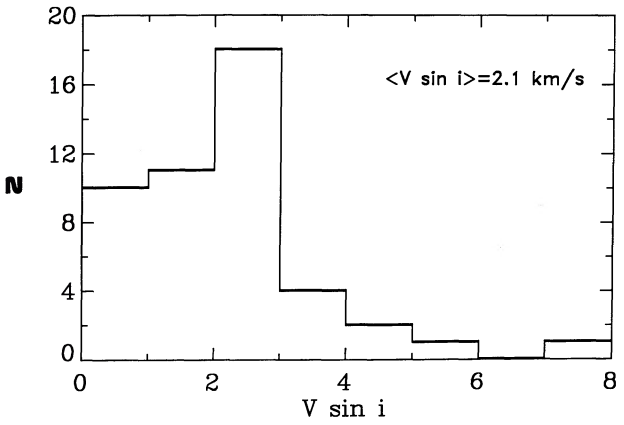

FIG. 4.—Histogram of measured $v \sin i$ for 47 M dwarfs in the solar neighborhood. Measurements below 3 km s^{-1} represent nondetections, owing to both random and systematic errors. The average $v \sin i$ is 2.1 km s^{-1}. But after correction for observational bias at $v \sin i = 0$, the true $\langle v \sin i \rangle \approx 1$ km s^{-1}, confirming the M dwarfs as the slowest rotators on the main sequence.

entirely at random from Joy & Abt (1974) based purely on accessibility from the northern hemisphere, brightness, and spectral type, and thus it serves as a representative (indeed nearly complete) sample of late-K and M dwarfs in the solar neighborhood. We note that EQ Vir was added to the sample after the initial selection process (because of its fast rotation) and so will be excluded from the statistics for the solar neighborhood. The average value of $v \sin i$ is found to be 2.1 km s^{-1}, after exclusion of EQ Vir. This average value lies below the meaningful detection threshold. Owing to the positive bias on $v \sin i$ measurements below 3 km s^{-1}, the true mean $v \sin i$ for these stars is surely less than 2.1 km s^{-1}, but a quantitative estimate of the bias effect on the mean $v \sin i$ is impossible. Based qualitatively on these errors and biases, it is clear that *the actual mean v sin i for late-K and M dwarfs in the solar neighborhood is less than* 2 km s^{-1}. If the true mean $v \sin i$ for M dwarfs *were* 2 km s^{-1}, we would have obtained a mean $v \sin i$ significantly greater than the 2.1 km s^{-1} found here. Thus the mean $v \sin i$ is certainly less than 2 km s^{-1}.

For comparison, one may consider a sample of slightly more massive dwarfs (K0–K8, $0.9 < B - V < 1.0$) in the solar neighborhood for which Soderblom (1985) has computed angular velocities from Ca II H and K measurements. Translating these to equatorial velocities and applying a statistical correction term of $\pi/4$ for inclination, one finds $\langle v \sin i \rangle = 1.3$ km s^{-1} for the expected average $v \sin i$ of K dwarfs. Apparently, the solar neighborhood M dwarfs, having $\langle v \sin i \rangle \approx 1$ km s^{-1}, rotate no more rapidly than the K dwarfs.

The mean $v \sin i$ of M dwarfs in several young open clusters are α Perseus $\langle v \sin i \rangle \approx 50$ km s^{-1}, Pleiades $\langle v \sin i \rangle \approx 50$ km s^{-1}, and Hyades $\langle v \sin i \rangle \approx 15$ km s^{-1}, having ages of 50, 70, & 600 Myr, respectively (Stauffer et al. 1987; Radick & Baliunas 1987; Stauffer 1991). Although the spread of $v \sin i$ values is large within each cluster, it is clear that at least half if not all M dwarfs lose considerable angular momentum during their early main-sequence lifetimes. If the α Perseus M dwarfs represent the characteristics of nearby M dwarfs when they were young, then the *surface* rotation decreases by a factor of about 50 during the main-sequence lifetime. Most of the mass and rotational inertia of an M dwarf resides in its convection zone where rotational coupling should be efficient, thus promoting solid body rotation. So it appears that many, if not all ZAMS M dwarfs suffer the loss of about 98% of their angular momentum during their main-sequence lifetimes.

4.3. *Zeeman Broadening*

Benz & Mayor (1984) have raised the possibility that significant line broadening in M dwarfs is due to unresolved Zeeman splitting of the lines. Saar (1987) has detected Zeeman effects in active dMe stars observed at 2.2 μm where Zeeman detectability is enhanced by about 4 times over that at visual wavelengths. But no Zeeman broadening has been detected in nonemission M dwarfs even in the IR, despite concerted efforts to do so (Saar 1990). We tested for the Zeeman effect here by searching for a correlation between line broadening and the Zeeman $g_{\rm eff}$ value which is proportional to the Zeeman splitting.

The four lines examined here have the following $g_{\rm eff}$ values: λ6126.2 (1.25), λ6141.7 (1.1), λ6085.2 (1.75), λ5703.5 (0.90), all based on LS-coupling theory. We included the two additional lines observed in the dMe star, EQ Vir, namely, λ6119.5 (1.1) and λ5590.1 (1.5). We formed a measure of enhanced line broadening given by $v \sin i / \langle v \sin i \rangle$, the ratio of $v \sin i$ for a given line to the average $v \sin i$ for that star. We expect that if the Zeeman effect is important, this ratio will correlate with the Zeeman $g_{\rm eff}$ value.

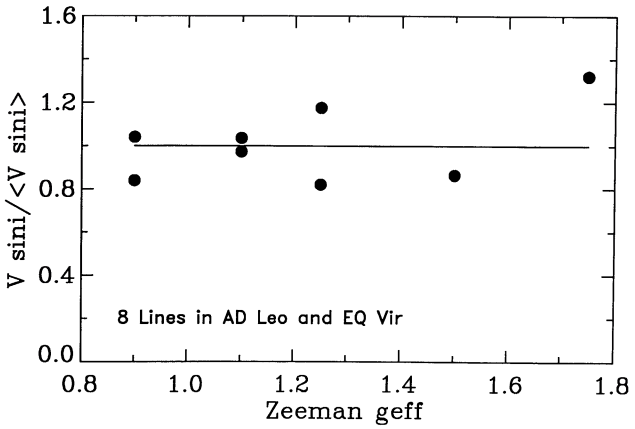

FIG. 5.—Test of the presence of Zeeman broadening in the lines used in this $v \sin i$ analysis. Ordinate shows the ratio of $v \sin i$ for a given line to the average for that star; abscissa is the Zeeman $g_{\rm eff}$ value. The lack of a clear trend indicates that Zeeman broadening is not significantly contaminating the rotation measurements.

Figure 5 shows a plot of this ratio versus $g_{\rm eff}$ for the eight lines measured in AD Leo and EQ Vir, the most magnetically active dMe stars in our sample. There is no convincing trend seen, although the most Zeeman sensitive line, λ6085 ($g_{\rm eff} = 1.75$), exhibits the largest $v \sin i$ enhancement over the average for its star, AD Leo. We consider Figure 5 to represent marginal evidence, at most, for Zeeman broadening in these two extremely active dMe stars. Thus, for the remaining 47 less active M dwarfs considered in the present sample, there can be no significant contamination of the measured rotational values by the Zeeman effect. Even for AD Leo and EQ Vir, the final values of $v \sin i$ cannot be significantly affected by Zeeman broadening since only one line shows even a suggestion of Zeeman enhancement. However, lines having $g_{\rm eff}$ greater than 2.0 in the optical region may exhibit significant Zeeman broadening for M dwarfs having widespread magnetic fields (Saar 1987; Marcy & Basri 1989).

5. CONCLUSIONS

We have refined a long-standing technique for determining $v \sin i$ in spectra of modest S/N ratio, namely, fitting lines with rotationally broadened lines of a nonrotating reference star. Even within the narrow range of spectral types considered here, dK5–dM5, line widths are correlated with mean equivalent widths, thus causing systematic errors of 2–3 km s^{-1} in measurements of $v \sin i$. We suppress this effect by employing a different nonrotating reference star for strong and weak-lined late-type stars. The subsequent determinations of $v \sin i$ then carry systematic errors of no more than 2 km s^{-1}, and random errors of about 1 km s^{-1}, for spectra having S/N $\approx$ 30. Past determinations of rotational broadening in M dwarfs carry similar systematic errors.

The application of this line-fitting analysis to 47 M dwarfs in the solar neighborhood yielded only three firm detections, namely, AD Leo (5.8 km s^{-1}), EQ Vir (8.3 km s^{-1}), Gliese 369 (4.8 km s^{-1}), and two probable detections, YZ CMi (4.8 km s^{-1}) and Gliese 569 (3.6 km s^{-1}). The other 42 M dwarfs

yielded only nondetections, carrying upper limits of 2–3 km s^{-1}, depending on the quality of the spectra. All nondetections were inactive dM dwarfs, as defined by Hα emission, thus confirming the rotational threshold for spot and chromospheric activity at about 5 km s^{-1}. On the other hand, four of the five stars with detected rotation (all but GL 369) exhibit flares or Hα in emission (Herbst & Layden 1987). This corroborates the paradigm that rotation induces magnetic fields which promote surface activity.

The average $v \sin i$ of M dwarfs in the solar neighborhood is about 1 km s^{-1}, after accounting approximately for the observational bias against $v \sin i < 0$. Thus local M dwarfs rotate no more rapidly than K dwarfs.

The present $v \sin i$ for AD Leo agrees with that of VSP, 5.8 and 5.0 km s^{-1}, respectively. Its photometric period permits an estimate of inclination, $33° < i < 44°$, suggesting that AD Leo is viewed somewhat pole-on. However, the photometric period, 2.7 days, of Spiesman & Hawley (1986) should be confirmed. For EQ Vir, there is modest agreement in $v \sin i$ between the present value (8.3 km s^{-1}) and that of Saar (9.25 km s^{-1} [1991, personal communication]), although VSP give 10.8 km s^{-1}. From the photometric periodicity, the rotation velocity at the equator is computed to be only 9.0 km s^{-1} (Pettersen 1989), less than the $v \sin i$ of VSP, which is impossible. Thus, either the rotation period of 3.96 days (or radius) is wrong by about 20% or the $v \sin i$ has been overestimated by VSP. Finally, the detection of rotation here for GL 569A further suggests that its age is no more than about 1 Gyr, as suggested by others. Thus its low-luminosity companion, GL 569B, remains as a candidate brown dwarf.

The measurement of rotation of late-type stars should not be done via line-broadening measurements such as attempted here. Even for the most rapidly rotating late-type stars such as EQ Vir, $v \sin i$ measurements are subject to modeling errors of at least 10%. Rather, rotation is better measured via photometric and chromospheric monitoring which provide not only superior rotational precision but also a wealth of information on the surface magnetic properties, such as spot characteristics, stellar cycles, and flares. The present work confirms that most late K and M dwarfs have rotation periods greater than 10 days. Measurement of rotation for these spectral types ($V > 8$ for virtually all) will require a 1 m, photometric telescope committed for at least 1 year to provide power spectra of adequate quality.

We thank J. Stauffer and S. Saar for contributions and critical comments; G. Basri, J. Valenti, and T. Misch for technical advice, and Richard Shine for the scientific analysis package, ANA. We acknowledge the support of NSF grant AST-8919634.

REFERENCES

Baliunas, S. L., et al. 1983, ApJ, 275, 752
Benz, W., & Mayor, M. 1984, A&A, 138, 183
Bopp, B. W., & Espanek, F. 1977, AJ, 82, 916
Bopp, B. W., & Fekel, F., Jr. 1977, AJ, 82, 490
Burrows, A., Hubbard, W. B., & Lunine, J. I. 1989, ApJ, 345, 939
Byrne, P. B., Doyle, J. G., & Menzies, J. W. 1985, MNRAS, 214, 119
Chugainov, P. F. 1974, Izv. Krzmskoj. Astrophys. Obs., 52, 3
Ferraz Mello, S., & Torres, C. A. O. 1971, Inf. Bull. Var. Stars, 577
Forrest, W. J., Skrutskie, M. F., & Shure, M. 1988, ApJ, 330, L119
Gliese, W., Jahreiss, H., & Upgren, A. R. 1987, in The Galaxy and the Solar System, ed. R. Smoluchowski, J. N. Bahcall, & M. S. Matthews (Tucson: Univ. of Arizona Press), 13
Gray, D. F. 1976, The Observation and Analysis of Stellar Photospheres (New York: John Wiley and Sons), 392
Hartmann, L. W., Hewett, R., Stahler, S., & Mathieu, R. D. 1986, ApJ, 309, 275
Hartmann, L. W., & Stauffer, J. 1989, AJ, 97, 873
Henry, T., & Kirkpatrick, J. D. 1990, ApJ, 354, L29
Herbst, W., & Layden, A. C. 1987, AJ, 94, 150
Joy, A. H., & Abt, H. A. 1974, ApJS, 28, 1
Kawaler, S. 1989, ApJ, 343, L65
Lacy, C. H. 1977, ApJS, 34, 479
Latham, D. 1985, in Stellar Radial Velocities, ed. A. G. D. Phillip & D. W. Latham (Schenectedy: Davis), 21
Marcy, G. W., & Basri, G. 1989, ApJ, 345, 480
Marcy, G. W., & Benitz, K. 1989, ApJ, 344, 441
Marcy, G. W., Lindsay, V., & Wilson, K. 1987, PASP, 99, 490
Mould, J. 1976, A&A, 48, 443
———. 1978, ApJ, 226, 923
Noyes, R. W., Hartmann, S. W., Baliunas, S. L., Duncan, D. K., & Vaughan, A. H. 1984, ApJ, 279, 763
Pettersen, B. R. 1983, in IAU Colloq. 71, Activity in Red-Dwarf Stars, ed. P. B. Byrne & M. Rodono (Dordrecht: Reidel), 17
———. 1989, A&A, 209, 279
Pettersen, B. R., Lambert, D. L., Tomkin, J., Sandmann, W. H., & Huang, L. 1987, A&A, 183, 66
Pinsonneault, M., Kawaler, S., & Demarque, P. 1990, ApJS, 74, 501
Prosser, C. F., Stauffer, J., & Kraft, R. P. 1991, AJ, 101, 1361
Radick, R. R., & Baliunas, S. L. 1987, in Fifth Cambridge Workshop on Cool Stars, Stellar Systems, and the Sun, ed. J. L. Linsky & R. E. Stencel (Berlin: Springer), 50
Saar, S. H. 1987, in Fifth Cambridge Workshop on Cool Stars, Stellar Systems, and the Sun, ed. J. L. Linsky & R. E. Stencel (Berlin: Springer), 10
———. 1990, Mem. Soc. Astron. Ital., 61(3), 559
Saar, S. H., Linsky, J. L., & Beckers, J. M. 1986, ApJ, 302, 777
Soderblom, D. R. 1983, ApJS, 53, 1
———. 1985, AJ, 90, 2103
Spiesman, W. J., & Hawley, S. L. 1986, AJ, 92, 665
Stauffer, J. 1991, in Proc. NATO Advanced Research Workshop on The Angular Momentum Evolution of Young Stars, ed. S. Catalano & J. Stauffer, in press
Stauffer, J., Giampapa, M. S., Herbst, W., Vincent, J. M., Hartmann, L. W., & Stern, R. A. 1991, ApJ, 374, 142
Stauffer, J., & Hartmann, L. W. 1986, ApJS, 61, 531
Stauffer, J., Hartmann, L. W., & Latham, D. 1987, ApJ, 320, L51
Tonry, J. L., & Davis, M. 1979, AJ, 84, 1511
Vaughan, A. H., Baliunas, S. L., Middlekoop, F., Hartmann, L. W., Mihalas, D., Noyes, R. W., & Preston, G. W. 1981, ApJ, 250, 276
Vogt, S. S. 1988, PASP, 99, 1214
Vogt, S. S., & Fekel, F. 1979, ApJ, 234, 958
Vogt, S. S., Soderblom, D. R., & Penrod, D. 1983, ApJ, 269, 250 (VSP)